OIKOS

*Research*

# Species-specific ontogenetic diet shifts attenuate trophic cascades and lengthen food chains in exploited ecosystems

**Jonathan C. P. Reum, Julia L. Blanchard, Kirstin K. Holsman, Kerim Aydin and André E. Punt**

*J. C. P. Reum (http://orcid.org/0000-0001-6601-4550) ✉ (reumj@uw.edu) and A. E. Punt, School of Aquatic and Fishery Sciences, Univ. of Washington, 1122 NE Boat St, Seattle, WA 98102, USA. – J. L. Blanchard, Inst. for Marine and Antarctic Studies, Univ. of Tasmania, Hobart, TAS, Australia. – K. K. Holsman and K. Aydin, Alaska Fisheries Science Center, National Marine Fisheries Service, NOAA, Seattle, WA, USA. JCPR and JLB also at: Centre for Marine Socioecology, Univ. of Hobart, TAS, Australia.*

**Oikos**
**128: 1051–1064, 2019**
doi: 10.1111/oik.05630

Subject Editor: Björn Rall
Editor-in-Chief: Dries Bonte
Accepted 14 January 2019

Ontogenetic diet shifts are pervasive in food webs, but rules governing their emergence and the implications for trophic cascades are only partly understood. Recent theoretical advances in multispecies size spectrum models (MSSMs) predict that the emergence of ontogenetic diet shifts are driven primarily by size-selective predation and changes in the relative abundances of suitably sized prey. However, these assumptions have not yet been tested with data. Here, we developed alternative MSSMs based on different assumptions about the nature of species and size-based preferences and tested them using an extensive dietary database for the Eastern Bering Sea (EBS). MSSMs with both size and species-specific prey preferences correctly predicted approximately three-fold more of the diet links than those that assumed fixed species preferences. Importantly, these model assumptions also had a profound effect on the strength of fishing-induced trophic cascades and the emergent trophic structure of the community with and without fishing. The diet-informed models exhibited lower predation mortality rates, particularly for small individuals (less than 1 g) which, in turn, reduced the intensity and reach of fishing-induced trophic cascades up the size spectrum. If the level and size dependency of piscivory observed in EBS predators is typical of other systems, the potential for fishing-induced trophic cascades may be over-stated in MSSMs as they are currently formulated and parameterized. Representation of species-specific ontogenetic shifts in diet can strongly influence system responses to perturbations, and the extensions we propose should accelerate adoption of MSSMs as frameworks for exploring size-based food web theory and developing modeling tools to support strategic management decisions.

Keywords: community ecology, ecosystem-based management, fisheries ecology, ontogeny, trophic interactions

## Introduction

Trophic cascades occur when a change in the abundance of individuals at one trophic level have attendant, alternating effects on abundances in adjacent levels. Although trophic cascades are recognized as an important phenomenon that can appear in a diversity of communities (Pace et al. 1999, Polis et al. 2000, Baum and Worm 2009),

NORDIC SOCIETY OIKOS

www.oikosjournal.org

our understanding of the processes that govern their occurrence, strength and reach in natural food webs is still evolving (Borer et al. 2005, Frank et al. 2007, Heath et al. 2014). In marine ecosystems, the harvesting of wild populations is a significant disturbance that can potentially trigger trophic cascades (Baum and Worm 2009). For instance, reductions in cod populations due to fishing in the Baltic Sea and Northeast Atlantic have been implicated in the release of their planktivorous prey which, in turn, crop larger quantities of zooplankton (Frank et al. 2005, Möllmann et al. 2008), and reductions in marine mammal abundances have triggered some of the most prominent examples of trophic cascades in benthic, nearshore ecosystems (Estes and Duggins 1995, Estes et al. 1998). At large spatial scales, inter-regional comparisons of predator and prey time series suggest that top–down trophic control (and potential for trophic cascades) may vary negatively with species richness and ocean temperature (Frank et al. 2007). However, quantitative modeling approaches remain essential tools for clarifying the potential for trophic cascades and generating predictions of the direct and indirect effects of human activities in specific ecosystems (Link 2010, Heath et al. 2014).

Common food web modeling methods entail developing descriptions of networks consisting of nodes (representing species or functional groups) linked by predator–prey interactions (Yodzis and Innes 1992, Williams and Martinez 2000, Brose et al. 2006). The models generally make the simplifying assumption that intrapopulation variation in prey composition or predator vulnerability can be ignored, which permits modeling of aggregate quantities such as total population biomass and production. While such species-based models have met some success as tools for evaluating trophic cascades and patterns of bottom–up and top–down control in a range of systems (Yodzis 1998, Daskalov 2002, Bascompte et al. 2005, Österblom et al. 2007), they have also received criticism for their failure to account for potentially complex ontogenetic trophic shifts within species (Nakazawa 2015). If species possess specialized life history stages but are parameterized as generalists at the species-level, food web models may overstate system robustness to species perturbations and removals (Rudolf and Lafferty 2011, Rudolf and Rasmussen 2013). Further, the models may be unable to resolve the trophic impacts of activities that alter the size distribution of populations. Fishing for instance may narrow the niche breadth of populations because large-bodied individuals, which tend to feed at higher trophic levels (Jennings et al. 2001), are disproportionately removed. Species-based food web models can be modified and species disaggregated according to life history stage or size class to account for ontogenetic diet shifts (Christensen and Walters 2004), but in practice this is usually done for a limited subset of species in the food web (Harvey et al. 2012, Geers et al. 2016).

Size spectrum models depict the abundance of individuals as a continuous function of body size (typically body mass) and arose through efforts to explain regularities in the size structure of aquatic ecosystems (Andersen et al. 2016, Guiet et al. 2016, Blanchard et al. 2017). The models recognize body mass as the fundamental attribute of an organism due to its outsized influence on physiological rates and ecological interactions. Initially, dynamic size spectra models ignored species identity and derived abundance–body mass predictions from individual-level processes governing predation, growth and mortality (Silvert and Platt 1980, Benoît and Rochet 2004, Shin and Cury 2004, Blanchard et al. 2009). At their core, the models represent the flow of individuals into size classes through somatic growth and track losses due to natural and fishing mortality. Predation is governed by size-structured feeding rules and somatic growth is based on the energy available from food intake after accounting for metabolism and reproduction. By scaling individual-level processes to the community-level, most parameters can be estimated from metabolic theory and the physiology of individual fish (Andersen et al. 2016).

Recent extensions to the general framework include representation of distinct predator species that can be differentiated by traits such as maturation and maximum sizes, feeding and growth rates and preferences for prey sizes and species (Hartvig et al. 2011, Maury and Poggiale 2013, Blanchard et al. 2014). Multi-species size spectrum models (MSSMs) include a more detailed physiological description of individual life histories than other modeling approaches that permit size and stage-structured diet shifts (e.g. Atlantis, Ecopath with Ecosim, Gadget; Persson et al. 2014) and their ability to represent species and their fisheries, which are inherently size-selective, make them useful tools for evaluating harvest tradeoffs and management strategies (Houle et al. 2012, 2016, Blanchard et al. 2014, Kolding et al. 2015, Zhang et al. 2016, Jacobsen et al. 2017). In previous MSSM simulation studies, removal of large individuals through fishing triggered damped oscillations down the size spectrum, analogous to the alternating changes in abundance with trophic level that typify top–down cascades in conventional food chain models (Andersen and Pedersen 2010, Houle et al. 2012, Rossberg 2012, Szuwalski et al. 2017).

Ontogenetic diet shifts and trophic dynamics in MSSMs emerge from rules governing size-based predation (Hartvig et al. 2011, Andersen et al. 2016). Predator diet composition is a function of the relative abundances of the prey encountered by a predator and the predator's prey size and species preferences (Fig. 1). In MSSMs, size preference is represented using a prey size selectivity function, or feeding kernel, and different prey species preferences are reflected in coefficients that effectively scale prey encounter rates. The prey species preference coefficients (herein termed 'prey species preferences') are invariant with predator size, and any emergent ontogenetic shifts in diet composition are driven by changes in the relative abundances of suitably sized prey (Hartvig et al. 2011). As represented in MSSMs, prey species preference can be conceptualized in a multitude of ways. For instance, these scaling coefficients have been parameterized to relate the potential effects of predator–prey species spatial overlap on prey encounter rates (Blanchard et al. 2014) and

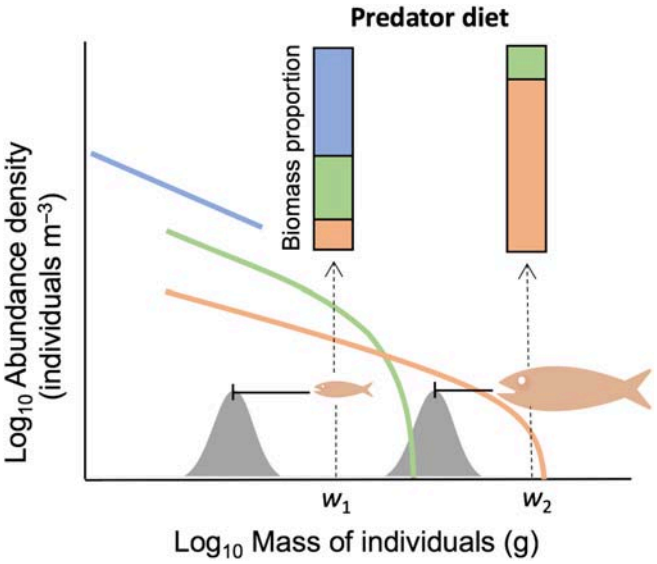


Figure 1. An overview of predation in multispecies size spectrum models (MSSMs). A background resource spectrum (blue) consisting of invertebrate prey and two fish population spectra (green and orange) are depicted. Suitably sized prey are determined using a feeding kernel (a log-normal prey size selectivity function). In the simplest case where prey species preferences of the predator do not differ, predator diet composition will reflect the relative biomasses of suitably sized prey. To illustrate, diet composition is depicted for the orange fish population at body mass $w_1$ and $w_2$ (note, cannibalism occurs). The grey bell curves correspond to the respective feeding kernels. Ontogenetic shifts in diet emerge because the relative biomasses of suitably sized prey change with predator body mass. Differences in preferences for prey species can change their representation in predator diets.

to scale prey encounter rates according to relative predation risk (Jacobsen et al. 2017).

Traditional approaches to food webs have focused on the role species-averaged traits such as body size and predator to prey body mass ratios have in determining the occurrence and strength of predator–prey interactions (Riede et al. 2011, Naisbit et al. 2012, Gravel et al. 2013), but intraspecific patterns have received less attention (reviewed in Brose et al. 2017). In contrast, size spectrum models originally focused on how dynamical, purely size-based interactions give rise to the size spectrum. With the introduction of MSSMs, intraspecific variation in predator diets can now be fully resolved within a dynamic food web modeling framework. Although there is experimental and observational evidence supporting aspects of the prey size-selection mechanism in MSSMs (Ursin 1973, Floeter and Temming 2003, Tsai et al. 2016), surprisingly, no attempts have been made to test model adequacy in relation to actual predator diets, thus leaving their level of realism with regard to ontogenetic diet shifts and the resulting trophodynamics an open question.

In the present study, we explicitly test the hypothesis that rules governing prey selection in MSSMs adequately capture predator–prey interactions in a real ecosystem. To do so, we calibrated MSSMs to the EBS, one of the most productive ecosystems in the world (Aydin and Mueter 2007), and utilized a wealth of fish predator diet data from an extensive ecosystem and fisheries monitoring program in the EBS (Livingston et al. 2017). We empirically test a core assumption in MSSMs, namely, that prey preference (i.e. the scaling of prey-specific encounter rates) is invariant with predator size. We do this by developing two sets of alternative MSSMs. The first model set consists of size-invariant prey species preferences that are derived from different assumptions about the processes influencing prey preference (Blanchard et al. 2014, Jacobsen et al. 2017, Szuwalski et al. 2017). Following the approach of previous studies, the models were calibrated to the EBS using biomass and catch data. For many fish predators, the assumption of size-invariant prey species preferences may not hold because prey encounter rates and capture success can change with ontogenetic shifts in morphology, behavior, feeding mode or habitat use (Werner and Hall 1988, Juanes et al. 2002, Mindel et al. 2016). We therefore developed a second set of MSSMs that contain a novel extension that enables size-varying prey species preferences. Diet data were used to tune the size-varying prey species preferences. All models were calibrated using data from one time period (1982–1991) and were projected forward using fishing mortality time series. The ability of the models to predict predator–prey interactions were evaluated for a later time period (2005–2014). We assess the consequences of these alternative prey species preference assumptions on ecosystem responses to fishing in terms of emergent trophic structure and trophic cascade strength and reach. If predator preferences for fish species are lower in diet-relative to nondiet-informed models, we would expect less top–down control and weaker fishing-induced trophic cascades.

## Material and methods

### Eastern Bering Sea MSSM

We developed an MSSM based on source code for the R package 'mizer' (Scott et al. 2014). The main equations that compose the MSSM are based on those of Hartvig et al. (2011) as implemented in 'R' by Blanchard et al. (2014) and Scott et al. (2014). The model code and necessary data are provided in an online repository along with scripts for stepping through the calibration procedure (<https://doi.org/10.6084/m9.figshare.7158635.v1>, Reum et al. 2018). Here, we provide an overview of the model and elaborate specifically on how predation is formulated. Full details of the EBS model formulation and parameterization are provided in Supplementary material Appendix 1.

Formally, the model provides predictions of the population dynamics of each species $i$ as described by its size spectrum, denoted $N_i(w)$, where $w$ corresponds to body mass (g).

The numerical density of individuals in the body mass range $w_1$ and $w_2$ is calculated from $\int_{w_1}^{w_2} N_i(w)dw$ and the total biomass density ($g\,m^{-3}$) of individuals is $\int_{w_1}^{w_2} N_i(w)wdw$. The size spectrum is obtained from a numerical solution of the classical McKendrick–von Foerster equation (Silvert and Platt 1978, Benoît and Rochet 2004):

$$\frac{\partial N_i(w)}{\partial t} + \frac{\partial g_i(w)N_i(w)}{\partial w} = -\mu_i(w)N_i(w) \quad (1)$$

where $g_i(w)$ is the somatic growth (g $year^{-1}$) and $\mu_i(w)$ the mortality ($year^{-1}$) of an individual with body mass $w$ (g). That is, $N(w)$ is obtained by considering growth to be balanced by mortality at all body masses. The mechanisms driving growth and mortality operate at the level of the individual and are integrated up to the population level using Eq. 1, thus circumventing the need for explicit individual-based simulations (Blanchard et al. 2017).

The above equation is supplemented with a boundary condition specifying how offspring join each population:

$$g_i(w_{0,i})N_i(w_{0,i}) = R_i \quad (2)$$

where $R_i$ is the reproduction of the offspring by mature individuals in species $i$ and $w_0$ is the body mass at birth of individuals. The numerical density of offspring is obtained from $R_i/w_{0,i}$ $R_i/w_{0,i}$. Recruitment of each predator follows a Beverton–Holt type stock–recruit relationship and recruitment occurs continuously throughout the year. Continuous recruitment results in species size spectra that are more stable relative to models with seasonally pulsed recruitment, but the aggregate community size spectrum remains relatively similar (Datta and Blanchard 2016). In addition to representing predator populations, the model also includes resource spectra to provide prey for the smallest sized predators and represent other food sources (Blanchard et al. 2009, Andersen et al. 2016). The model allows for species-specific traits that control growth rates, maturation, egg production, recruitment and maximum size, as described by equations in Supplementary material Appendix 1 Table A1 where, for consistency, we have retained the notation used in previous MSSM studies (Hartvig et al. 2011, Blanchard et al. 2014, Scott et al. 2014). Importantly, the model also includes species-specific prey species and size feeding preferences which govern emergent patterns in predator diets.

Conceptually, the predation process in MSSMs can be divided into two components, the first determines the proportional contribution of different prey species to predator diets and the second sets consumption rates. In the first component, the biomass of suitably sized prey is first obtained using a feeding kernel. Specifically, prey size preference is described using a log-normal selectivity function (Fig. 1). For clarity, we note that $w$ hereafter corresponds to predator body mass, $w_{prey}$ is prey body mass and that the subscripts $i$ and $j$ denote species-level parameters or functions with respect to predators and prey. For predator species $i$, size preference is a function of the body mass ratio of prey to predator ($w_{prey}/w$) following:

$$s_i(w_{prey}/w) = \exp\left[-\frac{\left(\ln(\beta_i w_{prey}/w)\right)^2}{2\sigma_i^2}\right] \quad (3)$$

where $s_i(w_{prey}/w)$ is the prey size preference, $\beta_i$ is the preferred predator to prey body mass ratio (that is, $w/w_{prey}$) that sets the peak of the feeding kernel, and $\sigma_i$ sets the feeding kernel width. The function represents the behaviorally and morphologically mediated choice of predators for prey when presented with prey of many sizes. Prey with body masses coinciding with the feeding kernel peak have a selectivity of 1. The biomass density of suitably sized prey available to the predator is obtained by integrating across the product of the feeding kernel and the biomass spectrum of prey species $j$, $N_j(w_{prey})w_{prey}dw_{prey}$. That is,

$$\varphi_{i,j}(w) = \int_0^\infty s_i(w_{prey}, w)N_j(w_{prey})w_{prey}dw_{prey} \quad (4)$$

where $\varphi_{i,j}(w)$ is the biomass density ($g\,m^{-3}$) of suitably sized prey. To account for a predator's prey species preference, $\varphi_{i,j}(w)$ is multiplied by the unitless scaling coefficient $\theta_{i,j}$ which can take any non-negative value. Assigning $\theta_{i,j}$ a value of 0 inhibits predation by predator species $i$ on prey species $j$ altogether. Note that in standard MSSMs, $\theta_{i,j}$ is not a function of predator body mass; prey species preference is constant with respect to predator body mass (Hartvig et al. 2011). At this stage, the proportional contribution of prey species $j$ to the diet of predator species $i$ in terms of biomass can be obtained from $\theta_{i,j}\varphi_{i,j}(w) / \Sigma_j \theta_{i,j}\varphi_{i,j}(w)$.

In the second component, actual consumption rates are based on the functional response of the predator and the volume search rate ($m^3$ $year^{-1}$), $V_i(w)$. The latter is described by the allometric relationship $\gamma_i w^q$. Positive values of $q$ indicate search rates increase with predator body mass and is assumed constant across species. However, $\gamma_i$ is calculated from observed species-specific growth rates as described by the von Bertalanffy growth function (VBGF; Scott et al. 2014). The derivation of $\gamma_i$ is based on several assumptions, including exclusive dependence by larvae on the background resource spectrum and specification of an initial feeding level. The resulting $\gamma_i$ values, in conjunction with appropriate values for other interlinked parameters (Scott et al. 2014), lead to growth that roughly approximates size-at-age patterns predicted by the VBGF under average feeding conditions (Blanchard et al. 2014). The available biomass (g $year^{-1}$) of prey species $j$ encountered by the predator, $E_{i,j}(w)$, follows:

$$E_{i,j}(w) = V_i(w)\theta_{i,j}\varphi_{i,j}(w) \quad (5)$$

and the biomass of all encountered prey species is:

$$E_i(w) = V_i(w)\Sigma_j \theta_{i,j}\varphi_{i,j}(w) \quad (6)$$

The form of Eq. 5 shows that $\theta_{i,j}$ can be viewed as a simple scaling coefficient for encounter rates of prey species $j$. The quantity of $E_i(w)$ ingested by the predator is obtained after considering satiation through a standard Holling type II functional response, where the feeding level $f_i(w)$ is calculated as:

$$f_i(w) = \frac{E_i(w)}{E_i(w) + I_{\max.i}(w)} \quad (7)$$

$I_{\max.i}(w)$ is the maximum consumption rate of the predator (g year$^{-1}$), and is described by the allometric relationship, $h_i w^n$ (for a species-specific derivation of $h$, Scott et al. 2014). Values of $f_i(w)$ range from 0 to 1, and the product of $f_i(w)$ and $I_{\max.i}(w)$ yields the biomass consumption rate (g year$^{-1}$) of the predator. Although other functional responses can conceivably be used in size spectrum models, the version described by Eq. 7 has been widely adopted in MSSMs (Hartvig et al. 2011, Blanchard et al. 2014, Scott et al. 2014, Andersen et al. 2016). Given the preceding relationships for consumption rates, predation mortality (year$^{-1}$) can be obtained following the equation specified in the Supplementary material Appendix 1 (Table 1A, Eq. B17; Hartvig et al. 2011 for the derivation).

Predation in our model version differs from the preceding description in regard to $\theta_{i,j}$, which can now be expressed as $\theta_{i,j}(w)$. That is, the prey species preferences can vary as a function of $w$. For clarity, we retain usage of $\theta_{i,j}$ when referring to size-invariant prey species preferences which are still supported in the model, but use $\theta_{i,j}(w)$ in relationship to size-varying prey species preferences. Two other significant changes to the original model code included separating the background resource spectrum into two distinct resource spectra to represent pelagic and benthic resources (Blanchard et al. 2009) and distinguishing sexes in instances where species showed strong sexual dimorphisms or sex-specific fishery selectivities. The latter was undertaken to better represent population size structure. Details of these modifications and their implementation in the model code are presented in Supplementary material Appendix 1.

The EBS model consists of 11 fish species, 3 fish functional groups and 3 crab species (Table 1). We included fish species based on their abundance in the region, data availability, and/or commercial value. We included snow crab, tanner crab and red king crab because they are abundant, support economically significant fisheries, and are important prey items for several fish species. Combined, the included predators accounted for ~95% of the community biomass based on estimates from annual bottom trawl surveys. Individuals from five fish predators (arrowtooth flounder, northern rock sole, flathead sole, yellow fin sole and Pacific halibut) and all crab species were partitioned according to sex to accommodate

Table 1. Predator groups included in the EBS model. $W_{max}$ is the maximum size of the predator group in the model. $F$ corresponds to average (1982–1991) full selection fishing mortality. Total biomass and spawner stock biomass (SSB) estimates (1982–1991 average) were obtained from stock assessments (Supplementary material Appendix 1 Table A3 for citation details). Asterisk denotes predator functional groups consisting of multiple species. For crabs, mature male biomass is indicated under SSB.

| Common name | Species name | Sex | $W_{max}$ (g) | $F$ (year$^{-1}$) | Total biomass (m tons) | SSB (m tons) |
|---|---|---|---|---|---|---|
| Alaska skate | *Bathyraja parmifera* | both | 21 401 | 0.019 | 353 594 | 71 688 |
| Arrowtooth flounder | *Atheresthes stomias* | female | 6953 | 0.028 | 298 414 | 141 181 |
| | | male | 2405 | 0.028 | | |
| Flathead sole | *Hippoglossoides elassodon* | female | 1692 | 0.037 | 648 047 | 123 179 |
| | | male | 900 | 0.037 | | |
| Northern rock sole | *Lepidopsetta polyxystra* | female | 1450 | 0.089 | 798 552 | 190 873 |
| | | male | 884 | 0.089 | | |
| Pacific cod | *Gadus macrocephalus* | both | 21 000 | 0.111 | 1 929 183 | 625 837 |
| Alaska plaice | *Pleuronectes quadrituberculatus* | both | 3232 | 0.050 | 697 879 | 301 365 |
| Walleye pollock | *Gadus chalcogrammus* | both | 4300 | 0.250 | 10 499 230 | 3 567 880 |
| Yellowfin sole | *Limanda aspera* | female | 1252 | 0.080 | 3 074 744 | 924 993 |
| | | male | 848 | 0.080 | | |
| Pacific halibut | *Hippoglossus stenolepis* | female | 37 536 | 0.335 | | |
| | | male | 14 504 | 0.335 | | |
| Sculpin* | | both | 5124 | 0.029 | 154 006 | |
| Forage fish* | | both | 79 | 0.000 | 1 985 160 | |
| Other flatfish* | | both | 2177 | 0.026 | 116 534 | |
| Snow crab | *Chionoecetes opilio* | female | 164 | 0.926 | 969 500 | |
| | | male | 1051 | 0.926 | | 241 130 |
| Tanner crab | *Chionoecetes bairdi* | female | 373 | 0.390 | | |
| | | male | 1738 | 0.390 | | 32 542 |
| Red king crab | *Paralithodes camtschaticus* | female | 2680 | 0.284 | | |
| | | male | 3661 | 0.284 | | 17 442 |

sex-specific fishery selectivities and notable sex-specific difference in maximum body size (Table 1).

Following previous MSSM studies, parameters controlling allometric relationships with standard metabolism, maximum consumption and search rate were held constant across species (Supplementary material Appendix 1 Table A2). Species- and sex-specific parameters related to growth rates and maturation and asymptotic sizes were obtained from stock assessments, other published sources or statistical analyses of biological data collected by the NOAA Alaska Fisheries Science Center (Supplementary material Appendix 1 Table A3). For a subset of parameters, values were chosen based on general knowledge of the trophic ecology of species. In particular, $\beta_i$ which governs the prey size preference of predators, was chosen based on the functional role of predators, similar to previous studies (Law et al. 2016, Szuwalski et al. 2017; Supplementary material Appendix 1 Table A3). For most species, size-dependent fishery selectivities were either sigmoidal or double-normal functions of body size, and parameters controlling their shape were available in stock assessments, estimated from information contained in the stock assessments, or obtained directly from assessment authors (Supplementary material Appendix 1 Table A5, A6). For the pelagic and benthic resource spectra, slope and intercept parameters were estimated from plankton and benthos functional groups represented in a regional biophysical model with 10 $km^2$ grid size resolution calibrated to the EBS (Hermann et al. 2016). Additional information on parameter estimation procedures are provided in the Supplementary material Appendix 1. Given the complexity of the model, its solution is obtained numerically (Andersen et al. 2016). The body mass axis was discretized on a $\log_{10}$ grid that spanned $10^{-6}$ to $10^4$ g. The grid was divided into 100 bins of equal interval on the $\log_{10}$ scale. The model was projected forward using a time step of 0.25 year (Blanchard et al. 2014). The model was insensitive to use of shorter time steps or smaller body mass intervals. Details of the numerical solution procedure are available in Andersen et al. (2016).

## Nondiet-informed models

The first model set consisted of three models with different $\theta_{i,j}$ parameterizations that correspond to different assumptions regarding the scaling of prey encounter rates. We refer to the model set as 'nondiet-informed'. The models (M) are as follows:

(M1) *Uniform prey preference.* Predators consume prey species in proportion to the relative abundances of suitably sized prey. This corresponds to setting all $\theta_{i,j}$ to 1 (Houle et al. 2016, Jacobsen et al. 2016, Szuwalski et al. 2017).

(M2) *Spatial overlap.* In this model $\theta_{i,j}$ are interpreted as scaling coefficients for the encounter rates of prey based on the level of predator–prey spatial overlap. An index conveying the proportion of individuals in the predator population exposed to individuals in the prey population are used for $\theta_{i,j}$ (Hartvig et al. 2011, Blanchard et al. 2014).

(M3) *Prey growth rate.* Here, $\theta_{i,j}$ are interpreted as scaling coefficients that reflect relative predation risk of prey species (Jacobsen et al. 2017). Fast growing prey species are assumed to forage for longer periods compared to slow growing species which, in turn, comes at the cost of increased relative exposure to (higher encounters with) predators. An index of relative growth rates is derived from von Bertalanffy growth function (VBGF) parameters of each prey species and are used to set $\theta_j$ (note we drop the subscript *i* because the index is the same across predator species of prey species *j*).

In the uniform model (M1), all values in the species preference array were set to 1. For the spatial overlap model (M2), Schoener's (1970) overlap index was calculated using numerical density estimates from annual bottom trawl survey data from the EBS. Trawl data were obtained from the Alaska Fisheries Science Center and the index was calculated following Kempf et al. (2010) and Blanchard et al. (2014). The index ranges between 0 and 1, with 0 corresponding to no shared spatial overlap and 1 indicting complete overlap.

Last, for the prey growth rate model (M3), VBGF parameters for individual prey species were used to calculate $\theta_j$. Specifically, the species-specific prefactor $h_j$ from the allometric relationship describing maximum consumption was used to obtain $\theta_j$. For species with growth patterns approximated by the VBGF, Hartvig et al. (2011) proposed obtaining $h_j$ following:

$$h_j = \frac{3K_j}{\alpha} W_{\mathrm{Inf}.j}^{1/3} \tag{8}$$

where $K_j$ and $W_{\mathrm{Inf}.j}^{1/3}$ are the von Bertalanffy growth rate and asymptotic body mass, respectively, and $\alpha$ is the assimilation efficiency (fixed across species). The *h* parameter sets the time scale of species, with high and low values corresponding to fast and slow growing species (Hartvig et al. 2011). Jacobsen et al. (2017) proposed relative values of $h_j$ be used as proxies for the relative vulnerability of species to predation, where

$$\theta_j = \frac{n}{\sum_n h} h_j \tag{9}$$

and *n* is the number of prey species.

## Diet-informed models

In the second model set, we used diet data to estimate the function $\theta_{i,j}(w)$. In principle, $\theta_{i,j}(w)$ may take any number of shapes depending on the specific assumption or hypothesis under consideration. Here, we used empirical diet data to directly inform the shape of $\theta_{i,j}(w)$. We provide a thorough description of the procedure in Supplementary material Appendix 1, but provide an overview here. Briefly, we obtained $\theta_{i,j}(w)$ using a two-stage approach.

In the first stage, a 'base model' that assumed size-invariant $\theta_{i,j}$ (M1, M2 or M3) was calibrated to 1980s biomass and catch data (see Model calibration). The calibrated model was projected to equilibrium, and the simulated predator diet compositions were obtained. Next, the ratio was obtained of the proportion of prey type *j* in the observed diets to the proportion in the simulated diets. Ratios greater than 1 indicate that the predator prefers the prey species *j* more than predicted by the base model, while values less than 1 indicate the opposite. The ratios were then modeled as a smooth spline function of predator body size. The fitted spline functions were used to predict ratios to all predator size classes, and the predicted values were multiplied by $\theta_{i,j}$ from the base model to obtain $\theta_{i,j}(w)$. Mean observed diet proportions used in the procedure were obtained by pooling diet data from individuals within the same $\log_{10}$ body mass bins used to discretized the body mass axis for obtaining the numerical solution of the model. Predators spanned $10^{-3}$ to $10^{4}$ g in body mass resulting in 71 body mass bins (Supplementary material Appendix 1 for diet data preprocessing and calculation details).

In the second stage, parameters controlling species recruitment were re-estimated (see Model calibration) but assuming $\theta_{i,j}(w)$. For predators lacking diet data (crabs, Alaska skate), size-invariant $\theta_{i,j}$ from the base model were retained. We attempted the procedure using M1–3 as base models and refer to the second model set (hereafter M4–6, respectively) as 'diet-informed'.

The two-stage method we used to tune $\theta_{i,j}(w)$ enabled us to avoid direct estimation of $\theta_{i,j}(w)$ through numerical optimization. Conceivably, a joint likelihood function could be developed that incorporates diet and biomass data and simultaneously estimates all parameters. However, the most recent MSSM versions (including the present version) are computationally demanding, and estimating more than 15–20 parameters through numerical optimization methods becomes increasingly infeasible given the time demand (Andersen et al. 2016). The additional number of parameters required for directly estimating $\theta_{i,j}(w)$ would exceed a hundred given the number of predator–prey linkages and the potential for strong nonlinearity.

## Model calibration

Following previous studies, the models were calibrated by tuning parameters controlling the maximum recruitment of species, $R_{\max.i}$ which effectively scales species abundances (Blanchard et al. 2014, Jacobsen et al. 2016, Szuwalski et al. 2017). That is, $R_{\max.i}$ corresponds to the maximum possible number of newly hatched individuals (individuals per volume, in this case $m^3$) a species can produce. Specifically, we compiled information on species catches, spawner stock biomasses (SSB) and population biomasses from individual species stock assessments or bottom trawl surveys (Table 1). For one important group (forage fish), system-wide biomass estimates were available from neither source, and a biomass estimate from a mass-balance model calibrated to the 1980s was utilized (Table 1). All biomass and catch estimates from a ten year period (1982–1991) were averaged and parameter estimation was performed by minimizing the sum of least squares between the log predicted and log average biomasses (either SSB, total biomass or both depending on availability of estimates) and catches using the quasi-Newton method with box constraints 'L-BFGS-B' in the *R* optimization function 'optim'. For fished species, the full selectivity fishing mortality (*F*) was set to values from stock assessments averaged over the same ten year period (Table 1). The models were run until equilibrium was reached as part of the parameter estimation procedure. For some of the models, oscillations emerged that stemmed from internal trophic dynamics. We therefore averaged biomasses and catches over a 25-year period after equilibrium or quasi-equilibrium was reached (Supplementary material Appendix 1 Fig. A2).

All three models showed strong linear relationships between observed and predicted mean 1980s biomasses and catches (Pearson's correlation coefficient, *R*: 0.94 and 0.99; Supplementary material Appendix 1 Fig. A1). To ensure the calibrated models produced plausible body growth and stock dynamics, we qualitatively compared simulated growth curves with empirical size-at-age data and examined time series of projected stock SSB and catches under historical fishing mortality rates and in reference to estimates from single species stock assessments. The calibrated models generated similar growth curves for predators (averaged over the calibration time period) that fell within the observed size-at-age data (Supplementary material Appendix 1 Fig. A3). Alaska skate, arrowtooth flounder, flathead sole, Alaska plaice and yellowfin sole growth curves were on the upper end of the observed range of size-at-age data, while the remaining species were closer to the median (Supplementary material Appendix 1 Fig. A3). The calibrated models also produced plausible and similar stock dynamics and catches when forced with historical fishing rates (Supplementary material Appendix 1 Fig. A4).

Of the diet-informed models, two were successfully calibrated (M5 and M6); predicted and observed catches and biomasses were highly correlated (*R*: 0.94–0.98; Supplementary material Appendix 1 Fig. A1). Convergence on stable $R_{\max}$ estimates for M4 was not possible despite restarting the optimization algorithm with different initial parameter values, longer spin-up times and the use of several other optimization algorithms. This was likely related to overly high predation rates resulting from assuming prey species preferences of 1 for Alaska skate which lacked diet data and was, in turn, prey to few other species. The diet-informed models also generated growth curves that were very similar to the nondiet-informed models (Supplementary material Appendix 1 Fig. A3) and produced plausible stock dynamics as well. Among species projections under historical fishing rates, walleye pollock, snow crab and tanner crab differed the most relative to the nondiet-informed model projections. Walleye pollock SSB and catch projections spanned approximately an order of magnitude across models, and oscillations were evident

in projections from model M5 (Supplementary material Appendix 1 Fig. A4, A5). M5 model projections for snow crab and tanner crab also exhibited oscillations, but projections from the remaining models were similar and relatively more stable (Supplementary material Appendix 1 Fig. A4). Relative to estimates from single species stock assessments, the models did not closely capture high frequency changes in SSB that were evident in some species (e.g. red king crab, walleye pollock, Pacific cod), but were more successful matching overall biomass trends, for instance, in Pacific cod, arrowtooth flounder, northern rock sole, yellowfin sole and red king crab (Supplementary material Appendix 1 Fig. A4).

Similar to other food web models, the calibrated MSSMs synthesize diverse types of information that varied in availability and quality for the represented species (Fulton et al. 2011). The calibration procedure was designed to reflect the relative biomass of the different species and used fishing mortality and biomass estimates from individual species assessments. This approach was preferred for computational efficiency and to avoid issues related to scaling ground trawl survey data since they frequently only cover a portion of the stock and a subset of sizes and/or ages. A similar approach was used in other MSSM studies (Blanchard et al. 2014, Jacobsen et al. 2017), recognizing issues such as specified or estimated natural mortality rates used in the assessment model.

### Model evaluation

For all models predictive performance in relationship to predator–prey interactions was evaluated following a pattern oriented modeling approach (Grimm et al. 2005). Specifically, we forced the calibrated models with historical time series of fishing mortality rates and compared predicted predator diets averaged over a decade (2005–2014) outside the calibration period to observations averaged over the same period. Two metrics of fit were calculated. First, for each predator species a measure of deviance explained ($R^2$) was calculated to assess overall model fit to empirical observations of diet data following $R^2 = (D_{null} - D_{res})/D_{null}$, where $D_{null}$ is the deviance from a null model wherein all prey groups are assumed to contribute equally to a predator species' diet across all body masses and $D_{res}$ is the deviance when diets are predicted by the size spectrum model. To accommodate proportions, the deviance based on the likelihood of the data was calculated assuming the data were Dirichlet distributed. Extremely poor model fits can result in negative $R^2$ values; a value of 1 indicates a perfect match between modeled and predicted diets. Mean observed diet proportions were calculated in the same manner as those used in the calibration procedure for the diet-informed models. For many species, sufficient data were generally available for body mass bins larger than 4 g. Second, the percentage of correctly predicted strong linkages between predators and their fish and crab prey was calculated. The measure emphasizes correct prediction of linkages that are more likely to influence predator–prey dynamics. We considered linkages strong and a positive match when both simulated and observed diet proportions were greater than 5%.

### Trophic cascades

We compared the strength of fishing-induced trophic cascades between models by first projecting the communities forward to equilibrium assuming no fishing mortality ($F = 0$). The unfished equilibrium communities were then projected forward but assuming $F$s corresponding to mean 2005–2014 levels until a new fished equilibrium was reached. We examined the relative change in equilibrium unfished and fished abundance size spectra. Fishing tends to target large-bodied individuals, so we anticipated that the ratio between abundance spectra (unfished/fished) would exceed 1 for the largest size classes. If fishing induces strong trophic cascades, we would also expect a prominent wave pattern in the abundance ratio extending down to smaller body size classes, the waves reflecting alternating changes in the abundances of predators and their smaller-bodied prey (Andersen and Pedersen 2010, Houle et al. 2012, Rossberg 2012). The strength and reach of the trophic cascades correspond to the wave amplitude and the level of damping down the size spectrum.

To compare trophic structure and clarify the importance of predation within the predator community across models, we calculated a relative measure of trophic level ($TL^{rel}$). Pelagic and benthic resource spectra prey were assigned a TL of 0. Consequently, predators that feed exclusively on pelagic or benthic resource spectra prey will have a $TL^{rel}$ of 1, and higher $TL^{rel}$ values indicate increased dependence on prey from the predator community. TL was calculated following Cortes (1999).

### Data deposition

Model R code and data used to parameterize the EBS models are available from Figshare: <https://doi.org/10.6084/m9.figshare.7158635.v1> (Reum et al. 2018).

## Results

### Multi-model evaluation

In general, the nondiet-informed models (M1, 2 and 3) all poorly predicted the diets of predators that fed heavily on fish and crabs based on strong prey linkages. For those predators (Pacific cod, Pacific halibut, walleye pollock and sculpin), average percentage of correctly assigned linkages ranged between 14 and 20% (Table 2). Average $R^2$ values were also poor: 0.41–0.55 (Table 2). In contrast, the diet-informed models (M5, 6) performed markedly better in terms of $R^2$ (averages: 0.80 and 0.82, respectively) and the percentage of correctly assigned prey linkages (averages: 67 and 49%, respectively; Table 2). Among individual predators, all showed improvements in both $R^2$ and the correct assignment of strong linkages between nondiet- and diet-informed

Table 2. Measures of fit to observed average predator diets (2005–2014) for nondiet-informed (M1–3) and diet-informed (M5, 6) EBS models. $R^2$ corresponds to the proportion of deviance explained by the model (extremely poor fits may result in negative $R^2$ values; 1 corresponds to a perfect fit. Strong links indicates the percentage of correctly predicted strong linkages between predators and their fish and crab prey and emphasizes correct assignment of links that are likely to influence predator dynamics. Values in bold indicate the best performing model for a given predator and performance measure. Predator superscripts indicate main prey of adults: 1, fish and crab; 2, pelagic and other benthic invertebrates.

| | $R^2$ | | | | | % Strong links (fish and crab prey) | | | | |
|---|---|---|---|---|---|---|---|---|---|---|
| Predator | M1 | M2 | M3 | M5 | M6 | M1 | M2 | M3 | M5 | M6 |
| Arrowtooth flounder[1] | −0.592 | −0.076 | −0.065 | 0.824 | **0.867** | 10.0 | 15.0 | 15.0 | **80.0** | **80.0** |
| Flathead sole[1] | 0.877 | 0.901 | 0.887 | 0.936 | **0.945** | – | – | – | – | – |
| Foragefish[2] | 0.834 | 0.814 | 0.833 | 0.902 | **0.902** | – | – | – | – | – |
| Pacific halibut[1] | 0.540 | 0.563 | **0.655** | 0.558 | 0.580 | 37.2 | 39.5 | 44.2 | 46.5 | **55.8** |
| Northern rock sole[2] | 0.914 | 0.857 | 0.905 | 0.982 | **0.983** | – | – | – | – | – |
| Other flatfish[2] | 0.951 | 0.951 | 0.946 | 0.996 | **0.997** | – | – | – | – | – |
| Pacific cod[1] | 0.648 | 0.662 | 0.683 | 0.853 | 0.896 | 6.1 | 15.2 | 21.2 | **90.9** | 72.7 |
| Alaska plaice[2] | 0.923 | 0.930 | 0.914 | **0.999** | 0.998 | – | – | – | – | – |
| Walleye pollock[1] | 0.748 | 0.751 | 0.751 | 0.913 | **0.925** | 0 | 0 | 0 | **80.0** | 0 |
| Sculpin[1] | 0.746 | 0.692 | 0.732 | **0.851** | 0.850 | 0.156 | 15.6 | 18.8 | **40.6** | 37.5 |
| Yellowfin sole[2] | 0.903 | 0.847 | 0.900 | 0.973 | **0.973** | – | – | – | – | – |
| Fish and crab eaters (mean) | 0.418 | 0.518 | 0.551 | 0.800 | **0.824** | 13.8 | 17.1 | 19.8 | **67.6** | 49.2 |
| Pelagic and benthic invertebrate eaters (mean) | 0.900 | 0.883 | 0.898 | 0.965 | **0.966** | | | | | |
| All predators (mean) | 0.681 | 0.717 | 0.740 | 0.890 | **0.901** | 13.8 | 17.1 | 19.8 | **67.6** | 49.2 |

models, with Pacific halibut being the lone exception with respect to $R^2$ (Table 2). The largest improvements in predictive performance were for Arrowtooth flounder; nondiet-informed $R^2$ values ranged from −0.59 to −0.065, but values for the diet-informed models were 0.82 and 0.87 (M5 and M6, respectively; Table 2). Similarly, the percentage of correctly assigned prey linkages increased from 10 to 15% in the nondiet-informed models to 80% in the diet-informed models (Table 2).

For predators that fed heavily on pelagic and benthic resource spectra prey (flathead sole, foragefish, northern rock sole, other flatfish, Alaska plaice, yellowfin sole), the improvement in diet predictive performance was more modest (Table 2). Average $R^2$ values ranged from 0.88 to 0.90 among the nondiet-informed models and were 0.96 and 0.97 for the diet-informed models (Table 2). Overall, M6 performed best in terms of $R^2$ averaged across all predators, but M5 performed better based on the average percent of correctly assigned strong prey linkages (Table 2).

All models generally captured a decrease in pelagic and increase in benthic resource spectrum prey with increasing predator size. The diet-informed models, however, were considerably better at predicting dome-shaped relationships between benthic resource spectrum prey proportions and predator mass (e.g. Pacific cod, Pacific halibut and arrowtooth flounder; Fig. 2). The diet-informed models also captured increased cannibalism with size in walleye pollock, the biomass-dominant predator in the EBS. Increased consumption of walleye pollock with size was also captured better for Pacific cod, Pacific halibut and arrowtooth flounder (Fig. 2). In general, nondiet-informed models overestimated the contribution of forage fish and yellowfin sole in the diets of smaller predators (less than ~100 g), but this was not the case for the diet-informed models (Fig. 2). The level of fit to diet data was poor for some predator–prey pairs regardless of model. For instance, forage fish were underrepresented in Pacific halibut diet across models (Fig. 2).

## Trophic cascades

Strong fishing-induced trophic cascades were apparent based on large alternating changes in the relative abundances of predators and their smaller sized prey (Fig. 3A). Trophic cascades were stronger in the nondiet-informed models and were more dampened in the diet-informed models where alternating changes in abundance attenuated more rapidly with decreasing predator size (Fig. 3A). The differences in pattern arise from different levels of predation across size classes at the community level (Fig. 3B). Relative to the diet-informed models, predation mortality in the nondiet-informed models is higher (maximum value: 12 versus 4 year$^{-1}$) over a larger range of body sizes (~$10^{-4}$ to $10^2$ versus ~1 to $10^2$ g; Fig. 3B). Consequently, top–down numerical control is higher and extends further up the size spectrum in the nondiet-informed models.

Overall, the maximum $TL^{rel}$ reached by predators in the diet-informed models was ~0.5 higher than in the nondiet-informed models, indicating a longer food chain and higher reliance in terms of biomass on prey from the predator community (Fig. 4). Moreover, whereas $TL^{rel}$ varied nonlinearly with body size for all predator species in the nondiet-informed models, the relationships were more linear and positive in the diet-informed models (Fig. 4). The relationship between $TL^{rel}$ and body size was also less fixed in the nondiet-informed models: under fished conditions, $TL^{rel}$ decreased ~0.25 in some body size classes. Changes in the diet-informed models were generally less than 0.1 across body sizes (Fig. 4).

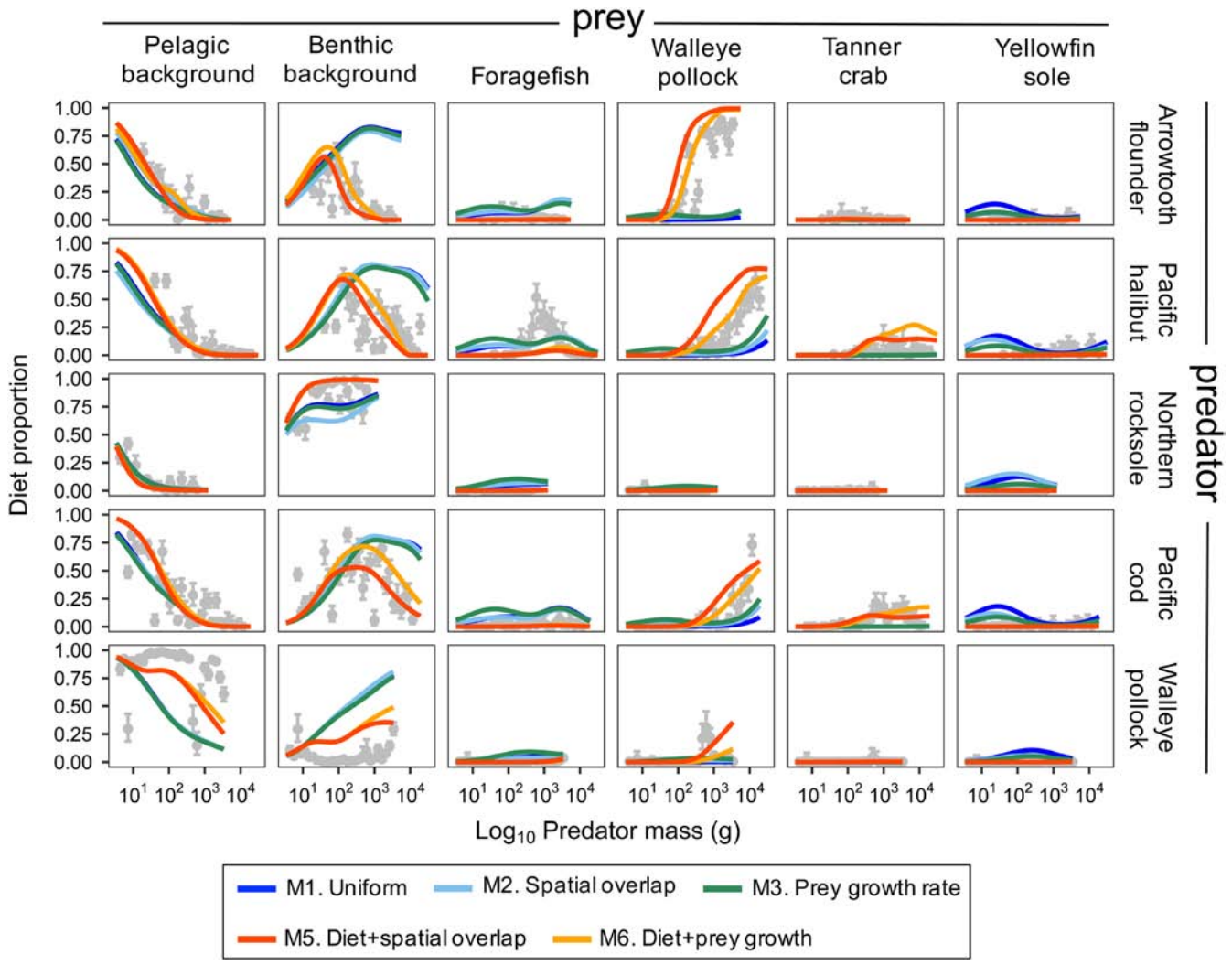


Figure 2. Examples of correspondence between out-of-sample modeled and observed diet proportions for a subset of predators and prey from the model. Closed grey circles are mean observed diet proportion; grey error bars indicate 95% confidence intervals. Diet observations and model predictions are averages for the 2005–2014 period.

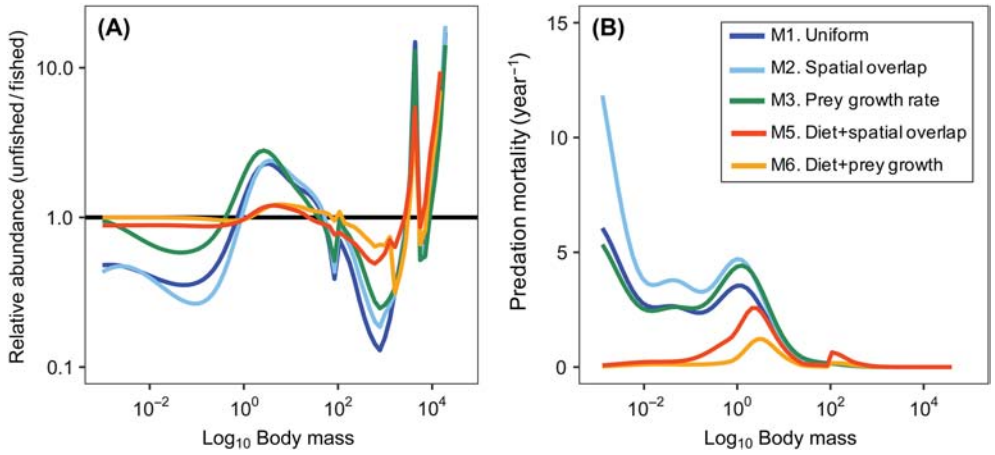


Figure 3. (A) Abundance spectra of equilibrium unfished communities relative to fished equilibrium communities (fishing mortality levels held constant at mean 2005–2014 levels). (B) Average predation mortality rates on fishes under equilibrium conditions (the average is weighted by species-specific abundances at size).

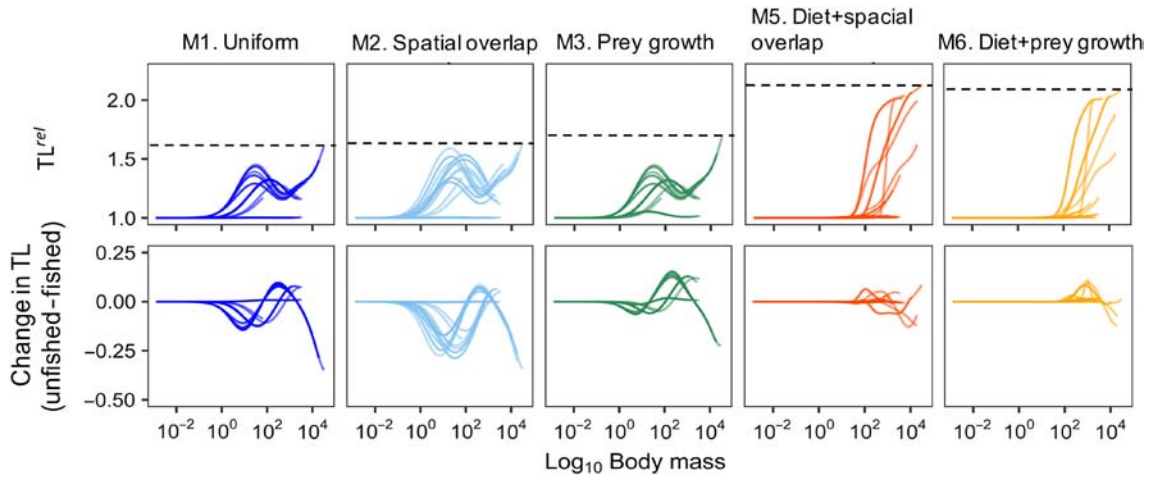


Figure 4. Top panel: relative trophic level of predator species as a function of body size under unfished conditions. Bottom panel: change in trophic level at size for predators between unfished and fished conditions. The dashed horizontal lines indicate the maximum relative trophic level reached by a predator species in each model.

## Discussion

MSSMs have gained popularity since their mathematical formalization as tools for representing real food webs, in part because prey selection is represented mechanistically, governed by only a few parameters, and does not depended on predator diet information (Andersen et al. 2016, Blanchard et al. 2017). However, as we show for the EBS, models that adopt simple prey preference scaling rules may yield emergent predator diets that correspond poorly to observations. Rather, the diet data support extending the prey selection theory underpinning MSSM to accommodate both size- and species-dependent prey preferences which, in turn, can lead to differing responses to fishing perturbations. We show that the reach and strength of fishing-induced trophic cascades are reduced substantially when species-specific ontogenetic shifts in prey preference are present in size-structured food webs. Further, other aspects of model behavior, including emergent predator $TL^{rel}$ and its response to fishing-induced shifts in the community, qualitatively differ depending on how prey preference is represented.

As conventionally structured, MSSMs predict strong fishing-induced trophic cascades (Andersen and Pedersen 2010, Houle et al. 2012, Rossberg 2012) which have even been evoked as a possible mechanism to explain reported fisheries catches for the East China Sea, a topic of intense debate (Szuwalski et al. 2017). If predation mortality rates are high over a range of size classes, as observed in all three nondiet-informed EBS models, the potential for top–down control exists and a trophic cascade can propagate down the size spectrum (Andersen and Pedersen 2010). In contrast, the diet-informed models indicated lower overall predation mortalities, and significant predation occurred only at body sizes larger than ~1 g, thus limiting the relative reach and strength of the trophic cascade. In shelf ecosystems, weak direct predation on small fish size classes by fish predators may be a more general phenomenon because many fishes (e.g. cottids, pleuronectids, gadids) have pelagic early life history stages, but forage more extensively near the seafloor and deepen their distribution as they grow (Mindel et al. 2016, Barbeaux and Hollowed 2017). Consequently, overlap in space, and thus encounter probabilities, may be lower than implied by assuming spatial overlap patterns based on larger individuals which are generally captured in bottom trawl surveys and that were used to parameterize M2. If similar patterns of piscivory hold in other shelf ecosystems, nondiet-informed MSSMs may systematically overestimate the indirect effects of fishing on community size structure. For instance, predicted increases in fishery yields resulting from the cascading effects of removing large-bodied predators may be overestimated if modelled top–down control through piscivory is stronger than conditions in the field (Andersen and Pederson 2010).

Inclusion of size and species-dependent prey preferences had two principle effects on trophic structure. First, longer food chains based on maximum $TL^{rel}$ values emerged in the diet-informed models because several species in the largest size classes relied more heavily on prey from the predator community. The higher reliance, however, did not result in stronger top–down control relative to nondiet-informed models because 1) heavy feeding on fish and crab was limited to predators in the largest but also least abundant size classes and 2) predation mortality was focused on a much narrower range of body sizes. Second, the emergent $TL^{rel}$ of predators was more stable in response to fishing perturbations, in part because the diet-informed prey species preferences implied higher levels of specialization than the nondiet-informed. This latter observation suggests that changes in trophic level metrics that reflect ecosystem status (e.g. mean community trophic level, cumulative trophic patterns; Cury and Christensen 2005, Link et al. 2015), will primarily be driven by species composition and size structure rather than through change in the trophic level of individuals themselves.

We have focused on the effects of size and species-specific prey preferences on trophic cascades within the predator community, but an important future task is to evaluate how trophic cascades propagate to other functional groups in the plankton and benthos. Fishing-induced trophic cascades can propagate down to phytoplankton and nutrients (Frank et al. 2007, Casini et al. 2008, Baum and Worm 2009), but the potential scope for trophic cascades in MSSMs are limited by the resolution of functional groups. For simplicity, non-fish groups are usually represented by background resource spectra that are either static or modeled dynamically (e.g. as a semi-chemostat or assuming logistic growth; Andersen et al. 2016). However, the MSSM framework is general and functional groups typified by different feeding modes, body size distributions, growth rates and life histories can be represented (Heneghan et al. 2016, Blanchard et al. 2017). For the EBS model, we explicitly represented three crab species, but including other benthic groups with substantially different feeding modes (e.g. suspension feeders, predatory polychaetes, carnivorous crustaceans) may be important because they compose a large fraction of fish diets. Inclusion of size and species-specific prey preferences as we propose should be useful for representing the biphasic (pelagic larval, demersal adult) feeding behavior common to many benthic animals and better capture their functional role as benthopelagic couplers.

We note that inclusion of size-dependent prey species preferences in MSSMs enables exploration of more general questions as well. For instance, it remains to be seen under what conditions size-dependent prey species preferences may increase trophic cascade strength or reach. A systematic evaluation of how different types of fisheries impact ecosystems composed of predators with varying degrees of ontogenetic shifts in prey preference would be a valuable exercise. Similarly, the implications of prey specialization by small (larval) predators (Young and Davis 1990) could also be explored if resource spectra are broken out into a wider range of functional groups. A goal of the present study was to calibrate an MSSM to a real ecosystem with special regard to predator–prey interactions, but food webs in other habitats (e.g. off-shelf pelagic ocean, coral reefs, estuaries, lakes) may differ in terms of species diversity and functional composition, and may therefore respond differently to fishing pressure.

The availability of diet data is remarkably high for the EBS (Livingston et al. 2011, 2017). If researchers wish to calibrate MSSMs to specific ecosystems which are diet data-limited, we suggest the development of multiple MSSMs with prey preference parameterizations that correspond to different plausible hypotheses. The shape and magnitude of size and species-specific prey preference functions could be set to reflect the hypothesized importance of size-dependent habitat shifts or levels of prey specialization. The calibrated model set could then be used to generate ensemble projections to better capture structural uncertainty (Hill et al. 2007). Alternatively, it may be possible to infer size and species preferences based on patterns in other systems. For instance, predator and prey traits such as body size, morphology, phylogeny, physiology, behavior and co-occurrence have been used to infer predator–prey linkages in food web networks (Gravel et al. 2013, Spitz et al. 2014, Rohr et al. 2016). Expanding these approaches to model and infer ontogenetic shifts in prey preference would be valuable for parameterizing MSSMs. We emphasize, however, that predator diet information will remain important for constraining model parameterization, validating predator–prey interactions, and reducing projection uncertainty, and should be a high research priority. That said, fish stomach content data have their own well-documented issues, including potential positive biases towards large prey and hard-bodied prey which take longer to digest (Hyslop 1980). Stable isotopes may offer an additional, alternative method for generating estimates of assimilated prey (Layman et al. 2012).

The theory underpinning MSSMs has evolved rapidly in the last decade (Blanchard et al. 2017), but critical tests of its ability to adequately capture predator–prey interactions in real ecosystems have lagged. For the first time, we show that standard assumptions embedded in the prey selection mechanism poorly predict important predator–prey interactions in a real food web. Instead, the diet data support modifying the mechanism to include both size and species-specific prey preferences. We show that revising MSSMs to do so has implications for model behavior with respect to fishing-induced trophic cascades. Our findings call for additional scrutiny in evaluating and testing predator–prey interactions in MSSMs, and suggest heightened caution is warranted when interpreting the outcomes of previous studies. While we have focused on improving predictions of trophic linkages in MSSMs, we note that other aspects of the framework also require additional careful consideration, particularly with regard to stock–recruitment relationships and parameters controlling reproductive efficiency (Andersen et al. 2016, Jacobsen et al. 2017). Ultimately, like other ecosystem models, broad-scale adoption of MSSMs for management applications will partly depend on confidence in their projections (Plagányi et al. 2014, Collie et al. 2016), and incorporating ontogenetic shifts in prey species preferences offers a promising direction for improving model adequacy.

*Acknowledgements* – We thank P. Woodworth-Jefcoats, A. Audzijonyte, C. Novaglio, K. Murphy, D. Gravel and J. Janelli for helpful comments on earlier versions of the manuscript.
*Funding* – This work is part of the Alaska Climate Change Integrated Modeling project (ACLIM) and was supported by grants through the NOAA National Marine Fisheries Service Fisheries and the Environment (FATE) program, the Stock Assessment Analytical Methods (SAAM) program, the Climate Regimes & Ecosystem Productivity (CREP), the Economics and Human Dimensions Program, the NOAA Alaska Fisheries Science Center, the NOAA Integrated Ecosystem Assessment Program (IEA), and the NOAA Research Transition Acceleration Program (RTAP). We also acknowledge support from the Australian Research Council Discovery Project DP170104240 ("Rewiring Marine Foodwebs").

## References


Andersen, K. H. and Pedersen, M. 2010. Damped trophic cascades driven by fishing in model marine ecosystems. – Proc. R. Soc. B 277: 795–802.

Andersen, K. H. et al. 2016. The theoretical foundations for size spectrum models of fish communities. – Can. J. Fish. Aquat. Sci. 73: 575–588.

Aydin, K. and Mueter, F. 2007. The Bering Sea – a dynamic food web perspective. – Deep Sea Res. II 54: 2501–2525.

Barbeaux, S. J. and Hollowed, A. B. 2017. Ontogeny matters: climate variability and effects on fish distribution in the eastern Bering Sea. – Fish. Oceanogr. 27: 1–15.

Bascompte, J. et al. 2005. Interaction strength combinations and the overfishing of a marine food web. – Proc. Natl Acad. Sci. USA 102: 5443–5447.

Baum, J. K. and Worm, B. 2009. Cascading top–down effects of changing oceanic predator abundances. – J. Anim. Ecol. 78: 699–714.

Benoît, E. and Rochet, M. J. 2004. A continuous model of biomass size spectra governed by predation and the effects of fishing on them. – J. Theor. Biol. 226: 9–21.

Blanchard, J. L. et al. 2009. How does abundance scale with body size in coupled size-structured food webs? – J. Anim. Ecol. 78: 270–280.

Blanchard, J. L. et al. 2014. Evaluating targets and tradeoffs among fisheries and conservation objectives using a multispecies size spectrum model. – J. Appl. Ecol. 51: 612–622.

Blanchard, J. L. et al. 2017. From bacteria to whales: using functional size spectra to model marine ecosystems. – Trends Ecol. Evol. 32: 174–186.

Borer, E. et al. 2005. What determines the strength of a trophic cascade? – Ecology 86: 528–537.

Brose, U. et al. 2006. Allometric scaling enhances stability in complex food webs. – Ecol. Lett. 9: 1228–1236.

Brose, U. et al. 2017. Predicting the consequences of species loss using size-structured biodiversity approaches. – Biol. Rev. 92: 684–697.

Casini, M. et al. 2008. Multi-level trophic cascades in a heavily exploited open marine ecosystem. – Proc. R. Soc. B. 275: 1793–1801.

Christensen, V. and Walters, C. J. 2004. Ecopath with ecosim: methods, capabilities and limitations. – Ecol. Model. 172: 109–139.

Collie, J. S. et al. 2016. Ecosystem models for fisheries management: finding the sweet spot. – Fish Fish. 17: 101–125.

Cortes, E. 1999. Standardized diet compositions and trophic levels of sharks. – ICES J. Mar. Sci. 56: 707–717.

Cury, P. M. and Christensen, V. 2005. Quantitative ecosystem indicators for fisheries management. – ICES J. Mar. Sci 62: 307–310.

Daskalov, G. M. 2002. Overfishing drives a trophic cascade in the Black Sea. – Mar. Ecol. Prog. Ser. 225: 53–63.

Datta, S. and Blanchard, J. L. 2016. The effects of seasonal processes on size spectrum dynamics. – Can. J. Fish. Aquat. Sci 73: 598–610.

Estes, J. A. and Duggins, D. O. 1995. Sea otters and kelp forests in Alaska: generality and variation in a community ecological paradigm. – Ecol. Monogr. 65: 75–100.

Estes, J. A. et al. 1998. Killer whale predation on sea otters linking oceanic and nearshore ecosystems. – Science 282: 473–476.

Floeter, J. and Temming, A. 2003. Explaining diet composition of North Sea cod (*Gadus morhua*): prey size preference vs. prey availability. – Can. J. Fish. Aquat. Sci. 60: 140–150.

Frank, K. T. et al. 2005. Trophic cascades in a formerly cod-dominated ecosystem. – Science 308: 1621–1623.

Frank, K. T. et al. 2007. The ups and downs of trophic control in continental shelf ecosystems. – Trends Ecol. Evol. 22: 236–242.

Fulton, E. A. et al. 2011. Lessons in modelling and management of marine ecosystems: the Atlantis experience. – Fish Fish. 12: 171–188.

Geers, T. et al. 2016. An original model of the northern Gulf of Mexico using ecopath with ecosim and its implications for the effects of fishing on ecosystem structure and maturity. – Deep Sea Res. II 129: 319–331.

Guiet, J. et al. 2016. Modelling the community size-spectrum: recent developments and new directions. – Ecol. Model. 337: 4–14.

Gravel, D. et al. 2013. Inferring food web structure from predator–prey body size relationships. – Methods Ecol. Evol. 4: 1083–1090.

Grimm, V. et al. 2005. Pattern-oriented modeling of agent-based complex systems: lessons from ecology. – Science 310: 987–991.

Hartvig, M. et al. 2011. Food web framework for size-structured populations. – J. Theor. Biol. 272: 113–122.

Harvey, C. et al. 2012. Food web structure and trophic control in Central Puget Sound. – Estuar. Coast. 35: 821 – 838.

Hill, S. L et al. 2007. Model uncertainty in the ecosystem approach to fisheries. – Fish Fish. 8: 315–336.

Heath, M. R. et al. 2014. Understanding patterns and processes in models of trophic cascades. – Ecol. Lett. 17: 101–114.

Heneghan, R. F. et al. 2016. Zooplankton are not fish: improving zooplankton realism in size-spectrum models mediates energy transfer in food webs. – Front. Mar. Sci 3: 321.

Hermann, A. J. et al. 2016. Projected future biophysical states of the Bering Sea. – Deep Sea Res. II 134: 30–47.

Houle, J. E. et al. 2012. Assessing the sensitivity and specificity of fish community indicators to management action. – Can. J. Fish. Aquat. Sci. 69: 1065–1079.

Houle, J. E. et al. 2016. Effects of seal predation on a modelled marine fish community and consequences for a commercial fishery. – J. Appl. Ecol. 53: 54–63.

Hyslop, E. J. 1980. Stomach contents analysis – a review of methods and their application. – J. Fish. Biol. 17: 411–429.

Jacobsen, N. S. et al. 2016. Comparing model predictions for ecosystem-based management 1. – Can. J. Fish. Aquat. Sci. 72: 1–11.

Jacobsen, N. S. et al. 2017. Efficiency of fisheries is increasing at the ecosystem level. – Fish Fish. 18: 199–211.

Jennings, S. et al. 2001. Weak cross-species relationships between body size and trophic level belie powerful size-based trophic structuring in fish communities. – J. Anim. Ecol. 70, 934–944.

Juanes, F. et al. 2002. Feeding ecology of piscivorous fishes. – In: Hart, P. J. B. and Reynolds, J. D. (eds), Handbook of fish biology and fisheries: fish biology, vol. 1. Blackwell, pp. 267–283.

Kempf, A. et al. 2010. The importance of predator–prey overlap: predicting North Sea cod recovery with a multispecies assessment model. – ICES J. Mar. Sci. 67: 1989–1997.

Kolding, J. et al. 2015. Maximizing fisheries yields while maintaining community structure. – Can. J. Fish. Aquat. Sci. 73: 644–655.

Law, R. et al. 2016. Balanced exploitation and coexistence of interacting, size-structured, fish species. – Fish Fish. 17: 281–302.

Layman, C. A. et al. 2012. Applying stable isotopes to examine food-web structure: an overview of analytical tools. – Biol. Rev. 87: 545–562.
Link, J. 2010. Ecosystem-based fisheries management: confronting tradeoffs. – Cambridge Univ. Press.
Link, J. S. et al. 2015. Emergent properties delineate marine ecosystem perturbation and recovery. – Trends Ecol. Evol. 30: 649–661.
Livingston, P. et al. 2011. Alaska marine fisheries management: advancements and linkages to ecosystem research. – In: Belgrano, A. A. and Fowler, C. C. (eds), Ecosystem based management for marine fisheries: and evolving perspective, Cambridge Univ. Press, pp. 113–152.
Livingston, P. A. et al. 2017. Quantifying food web interactions in the North Pacific – a data-based approach. – Environ. Biol. Fish. 100: 443–470.
Maury, O. and Poggiale, J. C. 2013. From individuals to populations to communities: a dynamic energy budget model of marine ecosystem size-spectrum including life history diversity. – J. Theor. Biol. 324: 52–71.
Mindel, B. L. et al. 2016. A trait-based metric sheds new light on the nature of the body size–depth relationship in the deep sea. – J. Anim. Ecol. 85: 427–436.
Möllmann, C. et al. 2008. Effects of climate and overfishing on zooplankton dynamics and ecosystem structure: regime shifts, trophic cascade and feedback loops in a simple ecosystem. – ICES J. Mar. Sci. 65: 302–310.
Nakazawa, T. 2015. Ontogenetic niche shifts matter in community ecology: a review and future perspectives. – Popul. Ecol. 57: 347–354.
Naisbit, R. E. et al. 2012. Phylogeny vs body size as determinants of food web structure. – Proc. R. Soc. B 279, doi:10.1098/rspb.2012.0327.
Österblom, H. et al. 2007. Human-induced trophic cascades and ecological regime shifts in the Baltic Sea. – Ecosystems 10: 877–889.
Pace, M. L. et al. 1999. Trophic cascades revealed in diverse ecosystems. – Trends Ecol. Evol. 14: 483–488.
Persson, L. et al. 2014. The ecological foundation for ecosystem-based management of fisheries: mechanistic linkages between the individual-, population- and community-level dynamics. – ICES J. Mar. Sci. 71: 2268–2280.
Plagányi, É. E. et al. 2014. Multispecies fisheries management and conservation: tactical applications using models of intermediate complexity. – Fish Fish. 15: 1–22.
Polis, G. A. et al. 2000. When is a trophic cascade a trophic cascade? – Trends Ecol. Evol. 15: 473–475.
Reum, J. C. P. et al. 2018. Data from: species-specific ontogenetic diet shifts attenuate trophic cascades and lengthen food chains in an exploited ecosystems. – <https://doi.org/10.6084/m9.figshare.7158635.v1>.
Riede, J. O. et al. 2011. Stepping in Elton's footprints: a general scaling model for body masses and trophic levels across ecosystems. – Ecol. Lett. 14: 169–178.
Rossberg, A. G. 2012. A complete analytic theory for structure and dynamics of populations and communities spanning wide ranges in body size. – Adv. Ecol. Res. 46: 427–521.
Rudolf, V. and Lafferty, K. D. 2011. Stage structure alters how complexity affects stability of ecological networks. – Ecol. Lett. 14: 75–79.
Rudolf, V. H. and Rasmussen, N. L. 2013. Ontogenetic functional diversity: size structure of a keystone predator drives functioning of a complex ecosystem. – Ecology 94: 1046–1056.
Rohr, R. P. et al. 2016. Matching-centrality decompsiton and forecasting of new links in networks. – Proc. R. Soc. B 283, doi:10.1098/rspb.2015.2702.
Schoener, T. W. 1970. Nonsynchronous spatial overlap of lizards in patchy habitats. – Ecology 43: 455–453.
Scott, F. et al. 2014. mizer: an R package for multispecies, trait-based and community size spectrum ecological modelling. – Methods Ecol. Evol. 5: 1121–1125.
Shin, Y. J. and Cury, P. 2004. Using an individual-based model of fish assemblages to study the response of size spectra to changes in fishing. – Can. J. Fish. Aquat. Sci. 61: 414–431.
Silvert, W. and Platt, T. 1978. Energy flux in the pelagic ecosystem: a time-dependent equation. – Limnol. Oceanogr. 23: 813–816
Silvert, W. and Platt, T. 1980. Dynamic energy-flow model of the particle size distribution in pelagic ecosystems. – Evol. Ecol. Zooplankton Commun. 3: 754–763.
Spitz, J. et al. 2014. Let's go beyond taxonomy in diet descriptions: testing trait-based approach to predator–prey relationships. – J. Anim. Ecol. 83: 1137–1148.
Szuwalski, C. S. et al. 2017. High fishery catches through trophic cascades in China. – Proc. Natl Acad. Sci. USA 114: 717–721.
Tsai, C. H., et al. 2016. Predator–prey mass ratio revisited: does preference of relative prey body size depend on individual predator size? – Func. Ecol. 30: 1979–1987.
Ursin, E. 1973. On the prey size preferences of cod and dab. – Meddelelser Fra Danmarks Fiskeriog Havundersogelser 7: 85–98.
Werner, E. E. and Hall, D. J. 1988. Ontogenetic habitat shifts in bluegill: the foraging rate-predation risk tradeoff. – Ecology 69: 1352–1366.
Williams, R. J. and Martinez, N. D. 2000. Simple rules yield complex food webs. – Nature 404: 180–183.
Yodzis, P. 1998. Local trophodynamics and the interaction of marine mammals and fisheries in the Benguela ecosystem. – J. Anim. Ecol. 67: 635–658.
Yodzis, P. and Innes, S. 1992. Body size and consumer–resource dynamics. – Am. Nat. 139: 1151–1175.
Young J. W and Davis, T. O. 1990. Feeding ecology of larvae of southern blue albacore and skipjack tunas (Pisces: Scombridae) in the eastern Indian Ocean. – Mar. Ecol. Prog. Ser. 61: 17–19.
Zhang, C. et al. 2016. An evaluation of implementing long-term MSY in ecosystem-based fisheries management: incorporating trophic interaction, bycatch and uncertainty. – Fish. Res. 174: 179–189.

Supplementary material (available online as Appendix oik-05630 at <www.oikosjournal.org/appendix/oik-05630>). Appendix 1.